Magnetically charged Euler-Heisenberg black holes with scalar hair

Thanasis Karakasis[●],[*] George Koutsoumbas,[†] Andri Machattou,[‡] and Eleftherios Papantonopoulos[§]

Physics Department, National Technical University of Athens, 15780 Zografou Campus, Athens, Greece

We study the Einstein-Euler-Heisenberg theory in the presence of a self interacting scalar field, minimally coupled to gravity. We solve analytically the field equations for the magnetically charged case and we obtain novel magnetically charged hairy black holes. The scalar field dresses the black hole with a secondary scalar hair. The hairy black hole develops three horizons when the Euler-Heisenberg parameter and the magnetic charge are small and the horizon radius is getting large when the scalar charge and the gravitational mass are large. The presence of matter and the magnetic field outside the horizon of the black hole increases the temperature only for small black holes. Calculating the heat capacity we show that the asymptotically anti–de Sitter (AdS) Euler-Heisenberg hairy black hole undergoes a second order phase transition and then it is stabilized. Also the weak energy condition is violated for the asymptotically AdS Euler-Heisenberg hairy black hole.

I. INTRODUCTION

The no-hair theorem states that black holes are described via charges that can be measured at infinity by an observer, and as a result there can be no additional degrees of freedom to characterize the black hole geometry. Hence, black holes are described by their mass, angular momentum and electromagnetic charges. The no-hair conjecture implies that a black hole spacetime does not allow degrees of freedom that are responsible for the formation of primary and secondary hair. The first ones are not associated with the conserved black hole parameters mentioned previously, while the second ones concern nontrivial fields that interact with the black hole parameters. The no-hair theorem affects all types of fields, such as scalar, gauge, tensor etc. We will only discuss the no-scalar hair theorem. The first proof of the no-scalar hair theorem was given by Bekenstein [1,2]. The main result is that a positive scalar potential such as a mass term potential cannot support a hairy black hole structure. As a result, if one wants to violate the no-hair theorem, a negative potential has to be considered for the scalar field [3].

The first hairy black hole which was an exact black hole solution with scalar field, called BBMB black hole, was found by Bocharova, Bronnikov and Melnikov and independently by Bekenstein [4]. However, it was found that the scalar field was divergent at the horizon and also the stability analysis showed that they were unstable [5], so these solutions were not physically acceptable. The

action of the BBMB black hole consists of the Ricci scalar, a scalar field with a kinetic term and a conformal coupling between matter and curvature. To cure the horizon-divergence problem, a cosmological constant was considered which is introducing a length scale, and a self interacting potential for the scalar field was considered at first [6] and exact de Sitter black holes were obtained with a regular scalar field at the horizon. However, the solutions turned out to be unstable again [7]. In [8] a scale in the form of nonlinear modification of gravity was introduced and the scalar field has been shown to be finite at the horizon. All these solutions consider a theory that is conformally invariant and there is a nonminimal coupling between matter and gravity.

Considering now the minimal coupling case, the first exact black hole solution was presented in [9], the Martinez, Troncoso, Zanelli (MTZ) black hole. The scalar potential is fixed *ad hoc*, the geometry of the solution is hyperbolic and the scalar field remains finite at the black hole event horizon. This solution was generalized with the presence of an electromagnetic field [10]. In [11], a potential that breaks the conformal invariance of the action of the MTZ black hole in the Jordan frame was considered and new black hole solutions where derived. In [12] the scalar field was fixed *ad hoc* and novel black hole solutions were investigated, letting the scalar potential be determined from the equations. The mass term comes as an independent integration constant and, as a result, the length scale introduced by the scalar field is a primary scalar hair. In [13] the electrically charged case was considered and in [14] the solution was generalized in the presence of nonlinear electrodynamics. In this case the mass has contributions from both an integration constant and the scalar length scale, so the scalar field dresses the black

[*]thanasiskarakasis@mail.ntua.gr
[†]kutsubas@central.ntua.gr
[‡]andrimachattou@hotmail.com
[§]lpapa@central.ntua.gr

hole with secondary hair. Static black holes with a charged scalar field and conformally invariant Maxwell electrodynamics in D dimensions have also been obtained numerically in [15]. The shadow of hairy rotating black holes in view of the results of the Event Horizon Telescope were discussed in [16] and in [17] the shadow of slowly rotating Gauss-Bonnet black hole with a dilaton field were investigated.

One can introduce several couplings between matter and curvature to evade the no-hair theorem, or consider modified theories of gravity. Couplings motivated from cosmology such as the nonminimal derivative coupling, i.e., a coupling between the Einstein tensor and the kinetic term of the scalar field have been investigated in [18–25]. These gravity theories are generated from the Horndeski class Lagrangian, leading to second order differential equations for the metric fields [26]. More black hole solutions regarding Horndeski Lagrangian can be found in Refs. [27–32]. The Gauss-Bonnet invariant coupled to the scalar field has been also considered where it was shown that the no-hair theorem can be evaded and asymptotically flat and anti–de Sitter (AdS) black holes carrying a scalar charge have been obtained [33–39], and $f(R)$ gravity black holes have also been discussed [46–48]. Couplings of the scalar field with electromagnetism has also been used to construct hairy black holes [40–45].

The Euler-Heisenberg Lagrangian of electrodynamics was at first considered in 1936 [49]. The Euler-Heinsenberg theory is a more accurate classical approximation of QED than Maxwell's theory, when the fields have high intensity. The vacuum is treated as a specific type of medium, and the properties of polarization and magnetization are determined by the clouds of virtual charges surrounding the real currents and charges [50]. A way to detect the effect of the Euler-Heisenberg theory has been proposed in [51]. Since the Euler-Heisenberg theory has interesting physical features, it was a natural consequence to couple the Euler-Heiseberg Lagrangian to the Ricci scalar via the volume element to search for black hole solutions. The first black hole solution to the Euler-Heisenberg electrodynamics was derived in [52], where analytical solutions were obtained for the magnetically charged case, also discussing electric charges and dyons. Electrically charged black holes were considered in [53] and [54], while in [54] the geodesic structure was the main study of the paper. In [55] motions of charged particles around the Euler-Heisenberg AdS black hole were studied. The thermodynamics of these black holes were studied in [56,57], while the quasinormal modes were calculated in [58]. Rotating black holes were found in [59,60], while the Euler-Heisenberg Lagrangian was introduced along with modified gravity theories in [61–63] and the corresponding black holes were analyzed. Finally, the shadow of the Euler-Heisenberg black hole was investigated in [64].

The Euler-Heisenberg theory describes accurately the behavior of electric and magnetic charges. However, in the presence of a strong gravitational field in a astrophysical environment, for example near the horizon of a astrophysical black hole, the electric charge is considered to be negligible due to the presence of plasma (electrically charged particles result in electrically conductive plasma) around astrophysical black holes that neutralizes any electric charge carried by the black hole. For the upper bounds of electric charge an astrophysical black hole can carry we refer to [65]. On the other hand, magnetically charged black holes cannot be neutralized with ordinary matter [66]. Recent astrophysical observations showed that many strong radio sources take the form of two emitting regions situated on opposite sites of a galaxy. To explain these astrophysical results a theory was proposed that the magnetic fields and high energy particles responsible for the synchrotron radiation were blown out of the galactic halo in a giant explosion. Then, a possible explanation was proposed that such explosions could be generated from gravitational collapse and a model was used presented in [67] which was composed by a configuration that contains only an electromagnetic field in a form of a collection of parallel magnetic lines which is held together by its own gravitational attraction known as a static Melvin Universe. This theory is described as a rigorous static cylindrically symmetric solution of the combined sourceless Einstein-Maxwell equations [68–70].

From the above discussion it would be very helpful to try to understand the behavior of a magnetic field in the presence of matter. The Euler-Heisenberg theory can provide a very reliable framework to study this effect. Motivated by this fact, in this work, we generalize the Einstein-Euler-Heisenberg black holes of [52] by introducing matter parametrized by a self interacting scalar field, minimally coupled to gravity. By assuming only magnetic charges, we integrate analytically the field equations and discuss the corresponding solutions. We found that when the Euler-Heisenberg parameter vanishes we obtain novel magnetically charged hairy black holes, while when the scalar charge vanishes, we get the solution of [52] while when both the Euler-Heisenberg parameter and the magnetic charge vanishes we go back to the well known hairy black hole solution of [12]. The scalar field dresses the black hole with secondary scalar hair, since the scalar charge is related to the mass parameter, while the scalar potential is negative in order to support the hairy structure and it possesses a mass term that satisfies the Breitenlohner-Friedman bound that ensures the perturbative stability of the AdS spacetime.

The black hole horizon shrinks as the magnitude of the scalar field is getting larger, while the horizon is getting larger as the gravitational mass is increasing. Calculating thermodynamical quantities we found that the presence of matter outside the horizon of the black hole and also the presence of the magnetic field increases the temperature for small black holes. We also found that the temperature

develops a minima in the AdS case signalizing in this way a second order phase transition, while the scalar field gains entropy for the black hole by the addition of a linear term in the entropy and hence the hairy black holes are thermodynamically preferred. Calculating the weak energy condition we find that it is violated in the case of asymptotically AdS spacetime.

The work is organized as follows. In Sec. II we set up the theory, derive the solution and discuss the effect of the scalar field on the black hole. In Sec. III we write down some limiting behaviors of the obtained black hole solution. In Sec. IV we discuss the thermodynamical properties, while in Sec. V we investigate the energy conditions and finally in Sec. VI we conclude.

II. BLACK HOLE SOLUTIONS

We consider the Euler-Heisenberg action in the presence of a scalar field

$$
S = \int d^4x \sqrt{-g}\mathcal{L}
$$
$$
= \int d^4x \sqrt{-g}\left(\frac{R}{2} - \frac{1}{2}\partial^\mu\phi\partial_\mu\phi - V(\phi) - P + \alpha P^2 + \beta Q^2\right),
$$
$$(1)$$

where $\mathcal{L}$ denotes the Lagrangian of the theory, $P = F_{\mu\nu}F^{\mu\nu}$, $Q = \epsilon_{\mu\nu\rho\sigma}F^{\mu\nu}F^{\rho\sigma}$, $F_{\mu\nu} = \partial_\mu A_\nu - \partial_\nu A_\mu$ is the Faraday tensor (field strength) and $\epsilon_{\mu\nu\rho\sigma}$ is the Levi-Civita tensor that satisfies

$$
\epsilon_{\mu\nu\rho\sigma}\epsilon^{\mu\nu\rho\sigma} = -24. \tag{2}
$$

The field equations are

$$
G_{\mu\nu} = T_{\mu\nu} \equiv T^\phi_{\mu\nu} + T^{\rm EM}_{\mu\nu}, \tag{3}
$$

$$
\Box\phi = \frac{dV}{d\phi}, \tag{4}
$$

$$
\nabla_\mu(F^{\mu\nu} - 2\alpha P F^{\mu\nu} - 2\beta Q \epsilon^{\mu\nu\xi\eta}F_{\xi\eta}) = 0, \tag{5}
$$

$$
T^\phi_{\mu\nu} = \partial_\mu\phi\partial_\nu\phi - \frac{1}{2}g_{\mu\nu}\partial^\alpha\phi\partial_\alpha\phi - g_{\mu\nu}V(\phi), \tag{6}
$$

$$
T^{\rm EM}_{\mu\nu} = 2F_{\mu\rho}F_\nu{}^\rho + \frac{1}{2}g_{\mu\nu}(-P + \alpha P^2 + \beta Q^2)
$$
$$
- 4\alpha P F_{\mu\rho}F^\rho_\nu - 8\beta Q \epsilon_{\mu\zeta\eta\rho}F^{\zeta\eta}F^\rho_\nu. \tag{7}
$$

We consider the following spherically symmetric ansatz for the spacetime metric

$$
ds^2 = -b(r)dt^2 + b(r)^{-1}dr^2 + b_1(r)^2 d\Omega^2, \tag{8}
$$

where $d\Omega^2 = d\theta^2 + \sin^2\theta d\varphi^2$ which allows us to consider the following electromagnetic ansatz for the four-vector A_μ

$$
A_\mu = (\mathcal{A}(r), 0, 0, Q_m \cos\theta), \tag{9}
$$

where Q_m is the magnetic charge of the black hole and the magnetic part of the four-vector will be null at the equatorial plane. Under these ansaetze, the scalar quantities P, Q that enter the field equations read

$$
P = \frac{2Q_m^2}{b_1(r)^4} - 2\mathcal{A}'(r)^2, \tag{10}
$$

$$
Q = -\frac{8Q_m\mathcal{A}'(r)}{b_1(r)^2}, \tag{11}
$$

where it is clear that Q will vanish if we do not consider dyons (both electric and magnetic charges).

The system of the field equations (3)–(7) admits an exact magnetically charged solution given by

$$
\mathcal{A}(r) = 0, \tag{12}
$$

$$
\phi(r) = \frac{1}{\sqrt{2}}\ln\left(1 + \frac{\nu}{r}\right), \tag{13}
$$

$$
b_1(r) = \sqrt{r(\nu + r)}, \tag{14}
$$

while the metric function $b(r)$ is obtained as

$$
b(r) = c_1 r(\nu + r) + \frac{(2r - c_2)(\nu + 2r) - 4Q_m^2}{\nu^2} + \frac{8\alpha Q_m^4(-\nu^2 + 12r^2 + 12\nu r)(\nu^2 + 3r^2 + 3\nu r)}{3\nu^6 r^2(\nu + r)^2} + \frac{2}{\nu^8}\ln\left(\frac{r}{\nu + r}\right)
$$
$$
* \left(-\nu^5 r(c_2 + \nu)(\nu + r) - 2Q_m^2 r(\nu + r)(\nu^4 - 24\alpha Q_m^2)\ln\left(\frac{r}{\nu + r}\right) + 48\alpha\nu Q_m^4(\nu + 2r) - 2\nu^5 Q_m^2(\nu + 2r)\right), \tag{15}
$$

where c_1, c_2 are constants of integration and ν is the scalar charge, also a constant of integration which determines the behavior of the scalar field. For a well behaved scalar field we will impose $\nu > 0$. At large distances, the metric function asymptotes to

$$b(r \to \infty) \sim 1 + \frac{-c_2 - \nu}{3r} + \frac{c_2\nu + \nu^2 + 6Q_m^2}{6r^2} + r^2\left(c_1 + \frac{4}{\nu^2}\right) + \frac{r(c_1\nu^2 + 4)}{\nu} - \frac{\nu(c_2\nu + \nu^2 + 10Q_m^2)}{10r^3} + \mathcal{O}\left(\left(\frac{1}{r}\right)^4\right). \quad (16)$$

We can see that the scalar charge ν is introducing a new scale in the theory which leads to the appearance of an effective cosmological constant. Also the generated mass term is given by both an integration constant and the scalar charge ν, hence the scalar field dresses the black hole with a secondary scalar hair. By redefining the integration constants, the asymptotic relation yields

$$b(r \to \infty) \sim 1 - \frac{2m}{r} + \frac{m\nu + Q_m^2}{r^2} - \frac{\Lambda_{\text{eff}} r^2}{3} - \frac{1}{3}r(\Lambda_{\text{eff}}\nu) - \frac{\nu(3m\nu + 5Q_m^2)}{5r^3} + \mathcal{O}\left(\left(\frac{1}{r}\right)^4\right), \quad (17)$$

where we have set $m = \frac{c_2 + \nu}{6}$ and $\Lambda_{\text{eff}} = -(3c_1 + \frac{12}{\nu^2})$. For small r the metric behaves as

$$b(r \to 0) \sim -\frac{8\alpha Q_m^4}{3\nu^4 r^2} + \mathcal{O}(r^{-1}), \quad (18)$$

from which we can deduce that the solution always describes a black hole at least in asymptotically flat or AdS spacetime, due to the fact that $b(r)$ is continuous and changes sign in the range $0 < r < \infty$. In the small scalar hair case ($\nu \to 0$), the metric function yields

$$b(r) = \left(1 - \frac{2m}{r} + \frac{Q_m^2}{r^2} - \frac{2\alpha Q_m^4}{5r^6} - \frac{\Lambda_{\text{eff}} r^2}{3}\right) + \nu\left(\frac{m}{r^2} + \frac{6\alpha Q_m^4}{5r^7} - \frac{Q_m^2}{r^3} - \frac{\Lambda_{\text{eff}} r}{3}\right) + \mathcal{O}(\nu^2). \quad (19)$$

Using the metric function (15) and the scalar field function (13) from the system of the field equations (3)–(7) we can specify the scalar potential

$$\begin{aligned} V(\phi) = \frac{1}{3\nu^8}(&\nu^8\Lambda_{\text{eff}}(\cosh(\sqrt{2}\phi) + 2) - 36m\nu^5(\sqrt{2}\phi(\cosh(\sqrt{2}\phi) + 2) - 3\,\sinh(\sqrt{2}\phi)) \\ &- 4\alpha Q_m^4 * (288\phi^2 + 2(72\phi^2 + 71)\cosh(\sqrt{2}\phi) - 432\sqrt{2}\phi\,\sinh(\sqrt{2}\phi) + 100\,\cosh(2\sqrt{2}\phi) \\ &- 14\,\cosh(3\sqrt{2}\phi) + \cosh(4\sqrt{2}\phi) - 229) + 6\nu^4 Q_m^2(8\phi^2 + 4(\phi^2 + 2)\cosh(\sqrt{2}\phi) \\ &- 12\sqrt{2}\phi\,\sinh(\sqrt{2}\phi) + \cosh(2\sqrt{2}\phi) - 9)). \end{aligned} \quad (20)$$

For small ϕ we have

$$V(\phi) \sim \Lambda_{\text{eff}} + \frac{\phi^2\Lambda_{\text{eff}}}{3} + \frac{\phi^4\Lambda_{\text{eff}}}{18} - \frac{4(\sqrt{2}m)\phi^5}{5\nu^3} + \mathcal{O}(\phi^6). \quad (21)$$

We can also express the potential as a function of r

$$\begin{aligned} V(r) = \frac{1}{6\nu^8 r^4(\nu + r)^4}\Big(&6\nu^6 Q_m^2 r^2(\nu + r)^2(\nu^2 + 12r^2 + 12\nu r) + \nu^6 r^3(\nu + r)^3(108m(\nu + 2r) + \Lambda_{\text{eff}}\nu^2(\nu^2 + 6r^2 + 6\nu r)) \\ &- 4\alpha\nu^2 Q_m^4(\nu^6 + 1332\nu^2 r^4 + 504\nu^3 r^3 + 30\nu^4 r^2 + 1296\nu r^5 + 432r^6 - 6\nu^5 r) \\ &+ 12r^3(\nu + r)^3\ln\left(\frac{r}{\nu + r}\right)\left(3m\nu^5(\nu^2 + 6r^2 + 6\nu r) + Q_m^2(\nu^2 + 6r^2 + 6\nu r)(\nu^4 - 24\alpha Q_m^2)\ln\left(\frac{r}{\nu + r}\right)\right. \\ &- 144\alpha\nu Q_m^4(\nu + 2r) + 6\nu^5 Q_m^2(\nu + 2r)\Big)\Big), \end{aligned} \quad (22)$$

and for small scalar hair ($\nu \to 0$):

$$V(r) = \Lambda_{\text{eff}} + \frac{\nu^2(25r^8\Lambda_{\text{eff}} - 18\alpha Q_m^4 + 25r^4 Q_m^2 - 30mr^5)}{150r^{10}} + \mathcal{O}(\nu^3). \quad (23)$$

As expected, at the zeroth order one obtains the cosmological constant. Its asymptotic behavior at large distances reads

$$V(r \to \infty) \sim \Lambda_{\text{eff}} + \frac{\Lambda_{\text{eff}}\nu^2}{6r^2} - \frac{\Lambda_{\text{eff}}\nu^3}{6r^3} + \mathcal{O}\left(\left(\frac{1}{r}\right)^4\right). \quad (24)$$

There is also a mass term in the potential

$$m^2 = V''(\phi = 0) = \frac{2}{3}\Lambda_{\text{eff}}, \quad (25)$$

which in the case of AdS spacetime is negative and the scalar field is a tachyon, however in this case it still respects the Breitenlohner-Freedman bound that ensures the perturbative stability of the AdS spacetime [71]. The Kretschmann scalar is singular at the origin

$$R_{\mu\nu\chi\psi} R^{\mu\nu\chi\psi}(r \to 0) \sim \frac{304\alpha^2 Q_m^8}{\nu^8 r^8} - \frac{7520(\alpha^2 Q_m^8)}{3\nu^9 r^7} + \mathcal{O}\left(\frac{1}{r}\right)^6, \quad (26)$$

while it is regular for any $r > 0$ and at infinity its behavior is

$$R_{\mu\nu\chi\psi} R^{\mu\nu\chi\psi}(r \to \infty) \sim \frac{8\Lambda_{\text{eff}}^2}{3} + \frac{2\Lambda_{\text{eff}}^2 \nu^2}{3r^2} + \mathcal{O}\left(\left(\frac{1}{r}\right)^3\right), \quad (27)$$

$$R_{\mu\nu\chi\psi} R^{\mu\nu\chi\psi}_{\Lambda_{\text{eff}}=0}(r \to \infty) \sim \frac{48m^2}{r^6} - \frac{8(18\nu m^2 + \nu^2 m + 12mQ_m^2)}{r^7} + \mathcal{O}\left(\frac{1}{r}\right)^8. \quad (28)$$

Thus the solution is valid for any $r > 0$ and describes a black hole in asymptotically (A)dS or flat spacetime for appropriate relations between the parameters. We will focus on the AdS case in order to make comparisons with the uncharged AdS hairy black hole and the flat case which is also of great interest. As can be seen from the definition of Λ_{eff} in order to obtain a flat spacetime the scale introduced by the presence of the scalar field has to be canceled by the integration constant c_1. In Fig. 1 we plot the metric function $b(r)$ and the potential $V(r)$ for the asymptotically AdS and flat spacetimes for a fixed scalar charge while changing α. The $\alpha = 0$ case differs in structure with the $\alpha \neq 0$ cases, having an inner horizon and an event horizon. The Euler-Heisenberg parameter α does not affect the horizon radius of the black hole as we can see. Moreover, the potentials are negative in order to support the hairy structure and violate the no-hair theorem. It is worth noting that, as we can see from the figures, α acts in favor of the no-hair theorem, since the existence of α ensures a negative potential everywhere, while for $\alpha = 0$ there is a small
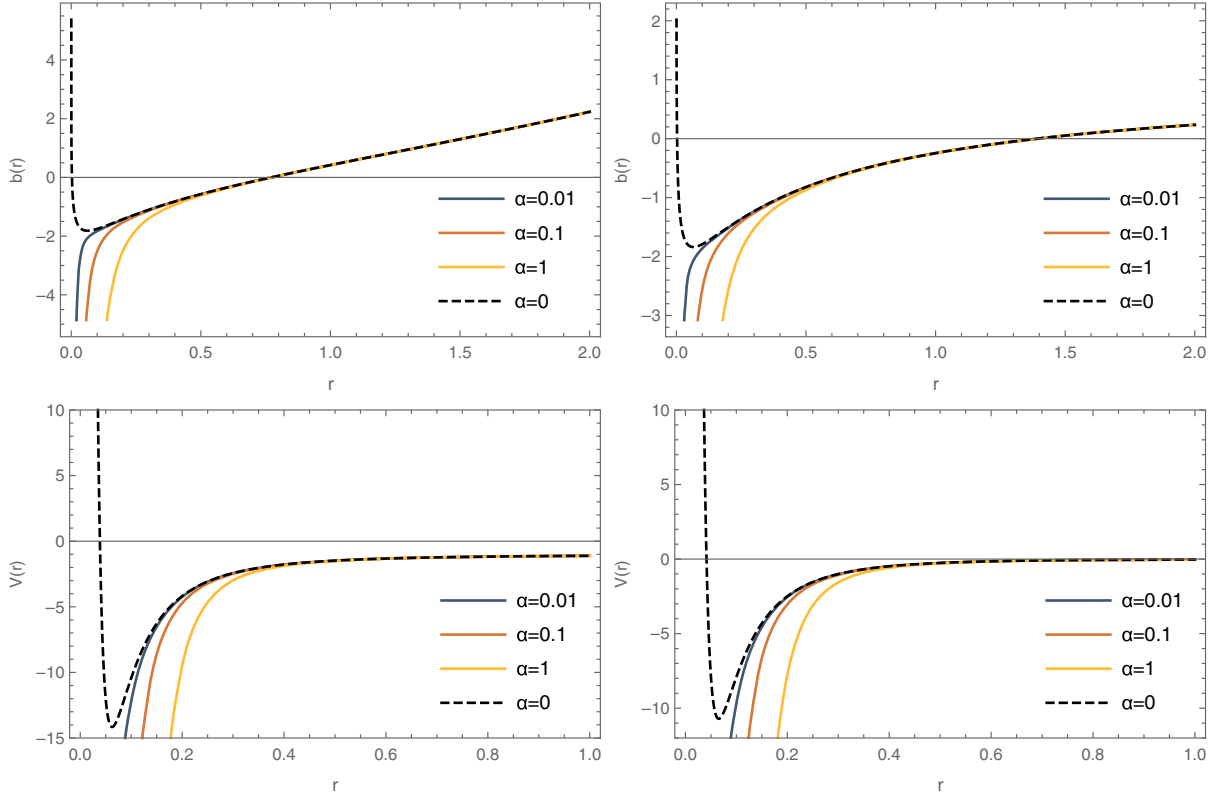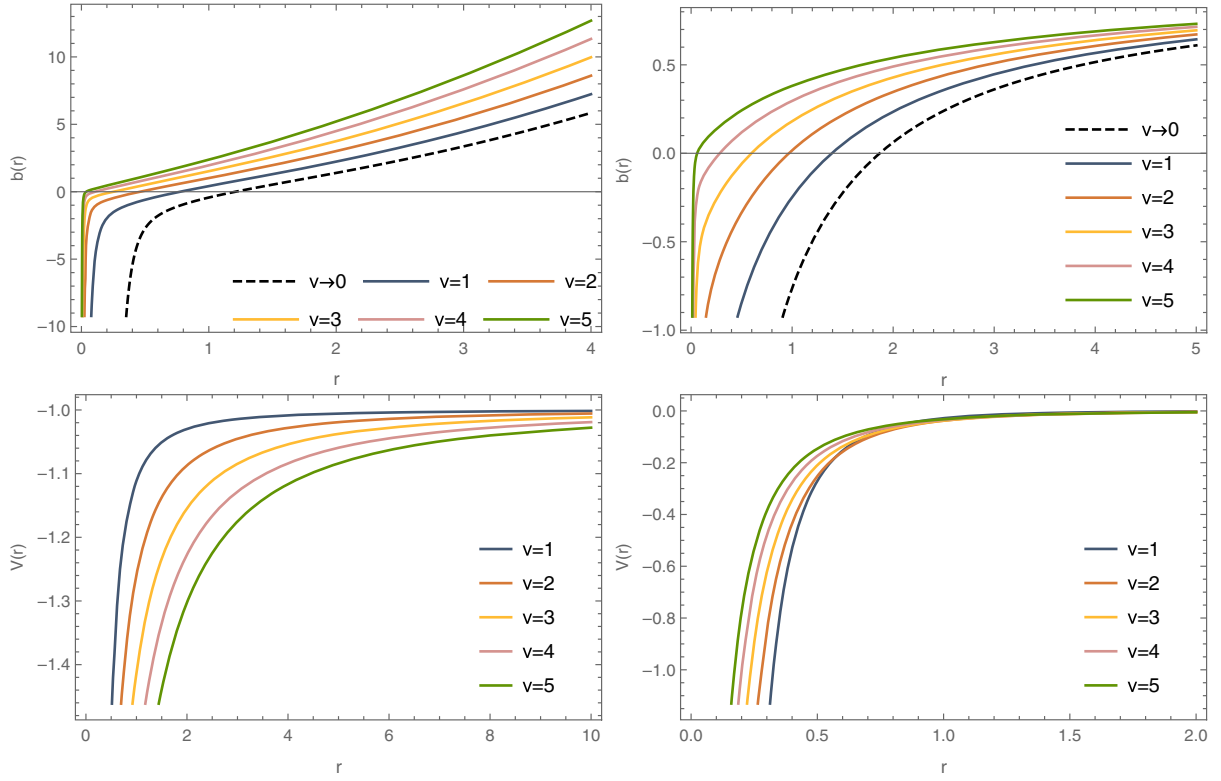

FIG. 1.   Hairy black hole configurations for asymptotically AdS $\Lambda_{\text{eff}} = -1$ (left) and flat $\Lambda_{\text{eff}} = 0$ (right) spacetimes, where we have fixed $m = 1$, $Q_m = 0.5$, $\nu = 1$, while changing the Euler-Heisenberg parameter α.

FIG. 2. Hairy black hole configurations for asymptotically AdS $\Lambda_{\text{eff}} = -1$ (left) and flat $\Lambda_{\text{eff}} = 0$ (right) spacetimes, where we have fixed $m = 1$, $Q_m = 0.5$, $\alpha = 0.5$, while changing the scalar charge ν.

region where the potential can be positive. In Fig. 2 we also plot $b(r)$, $V(r)$ while chancing ν having set $\alpha = 0.5$. We can see that for bigger ν (stronger scalar field) the black hole horizon radius is smaller. We also evaluate numerically and plot in Fig. 3 the horizon radius as a function of ν for both AdS and flat cases to visualize how the horizon changes as a function of the scalar charge.

To have a better understanding of the hairy Euler-Heisenberg black hole we found, we studied the horizon structure of the various solutions and their dependence on the gravitational mass. In Fig. 4 we show the dependence of

the horizons on the gravitational mass for $\Lambda_{\text{eff}} = 0$. The Euler-Heisenberg parameter is small ($\alpha = 0.05$) and the magnetic field is fairly large, $Q_m = 5$. We find that, in the interval of black hole masses between 5.5 and 8.0 (or 8.5), there are three possible solutions of the metric function, signaling one outer the two inner horizons. The influence of the scalar field is not large. The extreme solutions where we get just two horizons correspond to vanishing temperatures.

In Fig. 5 we show the horizon structures for asymptotically AdS spaces with ($\Lambda_{\text{eff}} = -1$). The Euler-Heisenberg
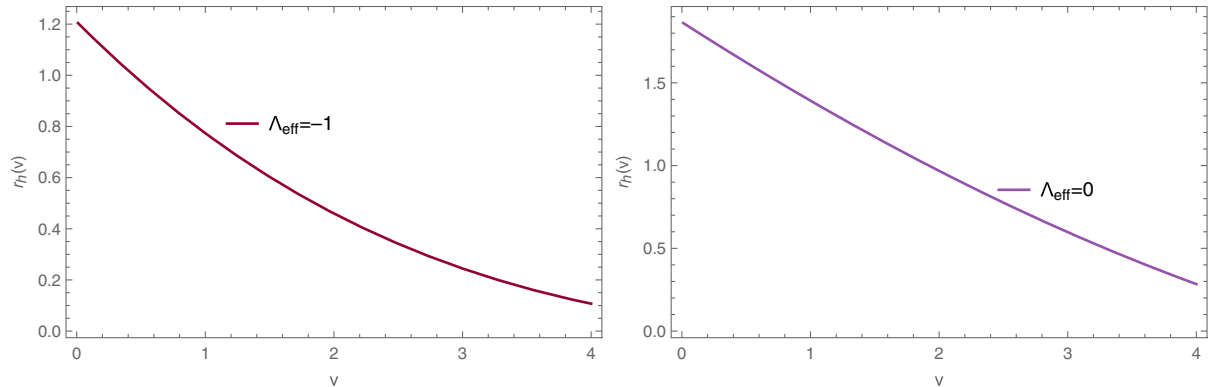

FIG. 3. The horizon radius r_h as a function of ν having set $m = 1$, $Q_m = 0.5$, $\alpha = 0.5$, for asymptotically AdS $\Lambda_{\text{eff}} = -1$ (left) and flat $\Lambda_{\text{eff}} = 0$ (right) spacetimes.
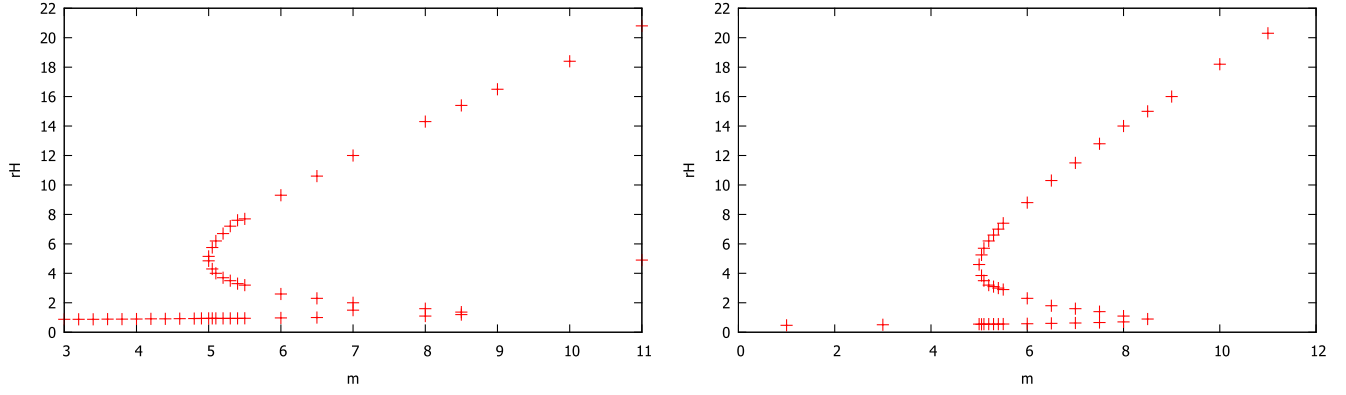
FIG. 4.   Horizons versus black hole mass. The asymptotically flat case ($\Lambda_{\text{eff}} = 0$) is depicted. The Euler-Heisenberg parameter α equals 0.05. Left panel: No scalar field ($\nu = 0$). Right panel: Small scalar field ($\nu = 1$).
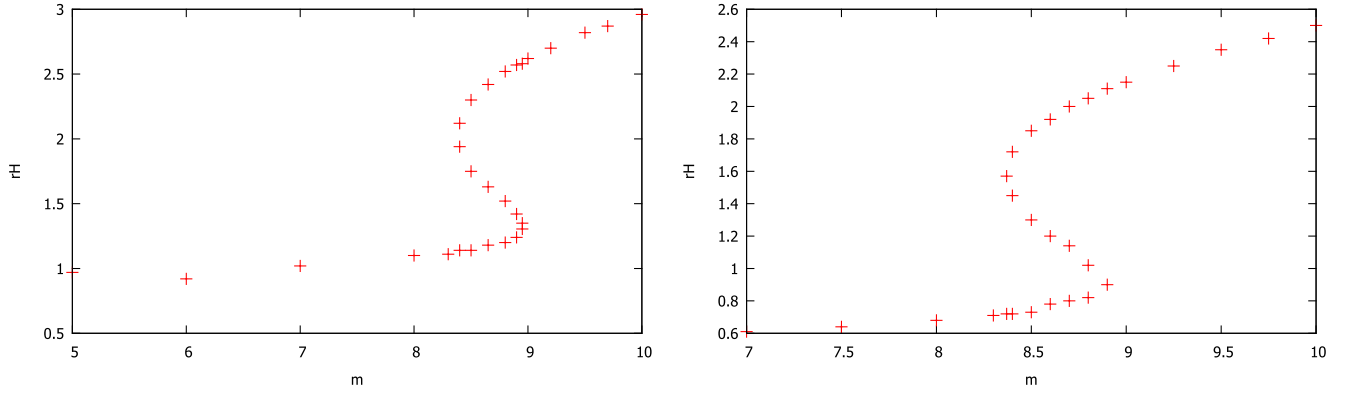

FIG. 5.   Horizons versus black hole mass. The asymptotically AdS case ($\Lambda_{\text{eff}} = -1$) is depicted. The Euler-Heisenberg parameter α equals 0.05. Left panel: No scalar field ($\nu = 0$). Right panel: Small scalar field ($\nu = 1$).

parameter is small ($\alpha = 0.05$) and the magnetic field is fairly large, $Q_m = 5$. We find that, in the interval of black hole masses between 8.5 and 9.0, there are three possible roots again. The influence of the scalar field is not large here either. We observe that the range of variation of the horizons is considerably smaller than the previous case: it varies between 1.0 and 3.5, which is an order of magnitude

smaller than before. The extreme solutions where we get just two solutions correspond to vanishing temperatures.

Finally in Fig. 6 we show once more the behavior of the horizons for a large scalar charge ($\nu = 10$). It contains both the asymptotically flat case and the asymptotically AdS case. We see the remarkable characteristic that the horizon (just one solution for each m) starts off with very small
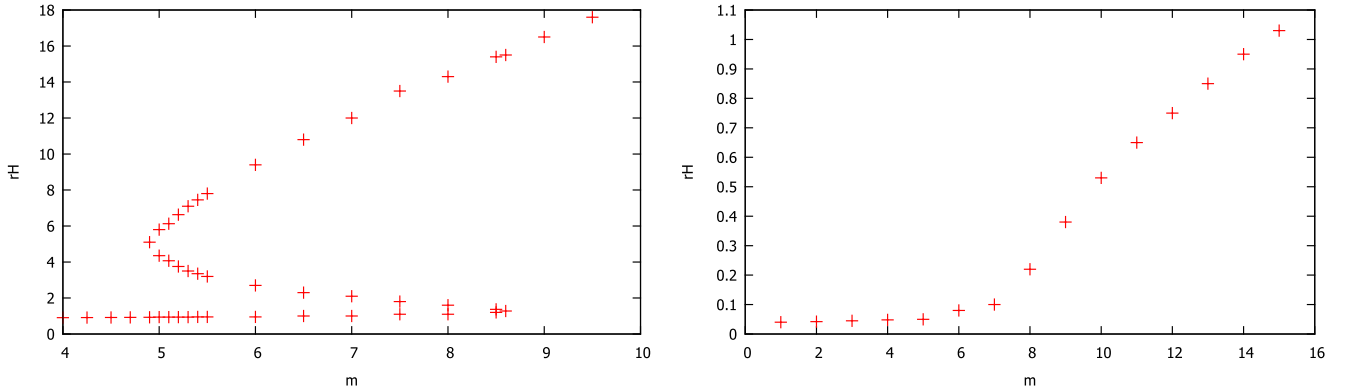

FIG. 6.   Horizons versus black hole mass. Large scalar field charge ($\nu = 10$). Left panel: Asymptotically flat case ($\Lambda_{\text{eff}} = 0$). Right panel: Asymptotically AdS case ($\Lambda_{\text{eff}} = -1$).

values, while, when m is large enough, it jumps to a much larger value. That is, a large black hole gets suddenly large horizon values. In addition, the horizon radii for $\Lambda_{\text{eff}} = -1$ are almost one order of magnitude smaller than the ones for $\Lambda_{\text{eff}} = 0$.

To summarize our results: The structure of three roots, as well as the existence of points with $T = 0$, appears when a is small. To have this behavior of the horizons, the magnetic charge Q_m should be large enough. The structure disappears when Λ_{eff} takes on large negative values. The horizon radius is getting large when the scalar charge and the gravitational mass are large.

The no-hair theorem by Bekenstein states that for an asymptotically flat spacetime, a positive definite potential cannot violate the no-hair theorem. For this reason we multiply the Klein-Gordon equation (4) by $V(\phi)$ and we integrate over the black hole exterior region

$$\int d^4x\sqrt{-g}(V(\phi)\Box\phi - V(\phi)V'(\phi))$$

$$= 0 \rightarrow \int d^4x\sqrt{-g}(\nabla_\mu(V(\phi)\nabla^\mu\phi)$$
$$- V'(\phi)\nabla_\mu\phi\nabla^\mu\phi - V(\phi)V'(\phi)) = 0. \quad (29)$$

For an asymptotically flat spacetime, we can ignore the first term which is a total derivative and this relation becomes

$$\int d^4x\sqrt{-g}V'(\phi)(\nabla_\mu\phi\nabla^\mu\phi + V(\phi)) = 0. \quad (30)$$

It is clear that the kinetic term above is always positive outside the black hole region. In order for the integral to be

zero, we want a negative potential in order to counterbalance the positive kinetic term, which will result in a zero area between the curve of the integrand and the r axis. The presence of the scalar field introduces a matter distribution outside the horizon of the black hole. The condition (30) guarantees that the kinetic energy of the scalar field has to counterbalance the potential energy of the scalar field in order to have a stable matter distribution outside the horizon of the black hole. Therefore we have to find regions of spacetime where the potentials are negative to violate the no-hair theorem and to support the hairy structure.

III. SPECIAL CASES FOR BLACK HOLE SOLUTIONS

In this section we will present special cases for the black hole solutions we found in the previous section depending on the choice of the parameters.

For the case $\nu \to 0$ we have the Euler-Heisenberg black hole [52]

$$b(r) = 1 - \frac{2m}{r} - \frac{2\alpha Q_m^4}{5r^6} + \frac{Q_m^2}{r^2} - \frac{\Lambda_{\text{eff}} r^2}{3}, \quad (31)$$

while the potential gives the cosmological constant $V = \Lambda_{\text{eff}}$. As it is expected, because the scalar field is decoupled, if we set the Euler-Heisenberg parameter equal to zero we can obtain the (A)dS RN spacetime, the magnetically charged RN spacetime by also setting $\Lambda_{\text{eff}} = \alpha = 0$, and the Schwarzschild one by further imposing $Q_m = 0$.

For the case $\alpha = 0$ we obtain novel magnetically charged hairy black hole solutions where the metric function is given by

$$b(r) = 1 - \frac{4Q_m^2}{\nu^2} - \frac{6m(\nu+2r)}{\nu^2} - \frac{1}{3}\Lambda_{\text{eff}} r(\nu+r) - \frac{4}{\nu^4}\ln\left(\frac{r}{\nu+r}\right)\left(3m\nu r(\nu+r) + \nu Q_m^2(\nu+2r) + Q_m^2 r(\nu+r)\ln\left(\frac{r}{\nu+r}\right)\right), \quad (32)$$

while the potential will be given by

$$V(\phi) = \frac{1}{3\nu^8}(\nu^8\Lambda_{\text{eff}}(\cosh(\sqrt{2}\phi) + 2) - 36m\nu^5(\sqrt{2}\phi(\cosh(\sqrt{2}\phi) + 2) - 3\sinh(\sqrt{2}\phi))$$
$$+ 6\nu^4 Q_m^2(8\phi^2 + 4(\phi^2 + 2)\cosh(\sqrt{2}\phi) - 12\sqrt{2}\phi\sinh(\sqrt{2}\phi) + \cosh(2\sqrt{2}\phi) - 9)). \quad (33)$$

For the case $\alpha = Q_m = 0$ we turn back to the well known asymptotically AdS black hole solutions with a scalar hair [12] where the metric function will be given by

$$b(r) = 1 - \frac{1}{3}r\Lambda_{\text{eff}}(\nu+r) - \frac{6m(\nu+2r)}{\nu^2} - \frac{12mr}{\nu^3}(\nu+r)\ln\left(\frac{r}{\nu+r}\right), \quad (34)$$

with potential

$$V(\phi) = \frac{1}{3}\Lambda_{\text{eff}}(\cosh(\sqrt{2}\phi) + 2) - \frac{12m(\sqrt{2}\phi(\cosh(\sqrt{2}\phi) + 2) - 3\sinh(\sqrt{2}\phi))}{\nu^3}. \quad (35)$$

IV. THERMODYNAMICS

In this section we will discuss the thermodynamical properties of the hairy black hole solution. We will study the temperature first. To do so we perform a Wick rotation $t \rightarrow -i\tau$, and move to Euclidean time. Imposing periodicity of the Euclidean time we can obtain the black hole temperature as

$$
T(r_h) = \frac{b'(r_h)}{4\pi}
$$

$$
\begin{aligned}
= -\frac{1}{12\pi\nu^5 r_h^3(\nu+r)^3(\nu(\nu+2r_h)+2r_h(\nu+r_h)\ln(\frac{r_h}{\nu+r_h}))} \Bigg(&-8\alpha\nu^2 Q_m^4(\nu^2-6r_h^2-3\nu r_h)(2\nu^2+6r_h^2+9\nu r_h) \\
&+ 12\nu^6 Q_m^2 r_h^2(\nu+r_h)^2 + \nu^6 r_h^3(\Lambda_{\text{eff}}\nu^2+12)(\nu+r_h)^3 \\
&+ 6r_h(\nu+r_h)\ln\left(\frac{r_h}{\nu+r_h}\right)\Bigg(\nu(\nu+2r_h)\Big(8\alpha Q_m^4(-\nu^2+6r_h^2+6\nu r_h)+\nu^4 r_h^2(\nu+r_h)^2\Big) \\
&- 2Q_m^2 r_h^2(\nu+r_h)^2(\nu^4-24\alpha Q_m^2)\ln\left(\frac{r_h}{\nu+r_h}\right)\Bigg)\Bigg),
\end{aligned}
\tag{36}
$$

where we have already substituted the mass parameter using the horizon condition $b(r_h) = 0$ and r_h denotes the event horizon. For small black holes, the Euler-Heisenberg parameter α plays a decisive role since

$$
T(r_h \ll 1) \sim \frac{4\alpha Q_m^4}{3\pi\nu^4 r_h^3} + \mathcal{O}\left(\frac{\ln(r_h)}{r_h^2}\right), \tag{37}
$$

while for large black holes the effect of α is negligible

$$
T(r_h \gg 1) \sim -\frac{\Lambda_{\text{eff}} r_h}{4\pi} - \frac{\Lambda_{\text{eff}}\nu}{8\pi} + \frac{\Lambda_{\text{eff}}\nu^2+20}{80\pi r_h} + \mathcal{O}\left(\frac{1}{r_h^2}\right). \tag{38}
$$

We can see this behavior in Fig. 7 where we plot the temperature of the black hole while changing the Euler-Heisenberg parameter α. We observe that α increases the temperature in the case of small black holes. In Fig. 8 we plot the black hole temperature having fixed the Euler-Heisenberg parameter $\alpha = 0.5$, while we vary the scalar charge of the solution both for asymptotically AdS and flat cases. The temperature of the asymptotically AdS case develops a minimum which can be obtained numerically. For example for $Q_m = 0.5$, $\alpha = 0.5$, $\nu = 1$, $\Lambda_{\text{eff}} = -1$ we find that $T'(r_h^{\min}) = 0 \rightarrow r_h^{\min} = 0.543748$ which corresponds to $T(r_h^{\min}) = 0.147635$.

The entropy of the black hole may be obtained using Wald's formula [72] which for our action reads

$$
S(r_h) = -2\pi \oint d^2x \sqrt{h}\left(\frac{\partial\mathcal{L}}{\partial R_{\alpha\beta\gamma\delta}}\right)\Bigg|_{r=r_h} \hat{\epsilon}_{\alpha\beta}\hat{\epsilon}_{\gamma\delta}, \tag{39}
$$

where $\hat{\epsilon}_{\alpha\beta}$ is the binormal to the horizon surface normalized to satisfy $\hat{\epsilon}_{\alpha\beta}\hat{\epsilon}^{\alpha\beta} = -2$ and h is the induced metric on the horizon. Since the only quantity in the Lagrangian that involves the Riemann tensor is the Ricci scalar, we can obtain the standard Bekenstein-Hawking area law [73]
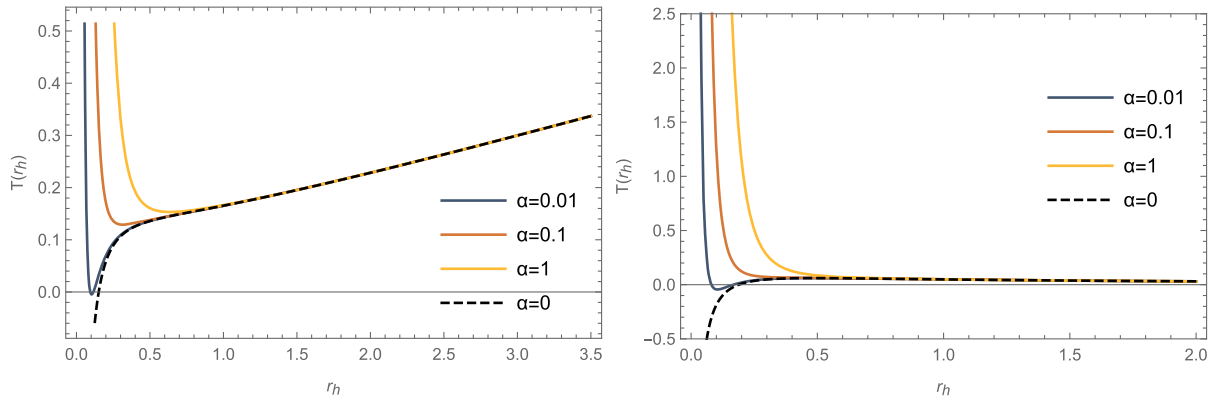

FIG. 7. The temperature of the hairy black hole configurations for asymptotically AdS $\Lambda_{\text{eff}} = -1$ (left) and flat $\Lambda_{\text{eff}} = 0$ (right) spacetimes, where we have fixed $Q_m = 0.5$, $\nu = 1$, while changing the Euler-Heisenberg parameter α.
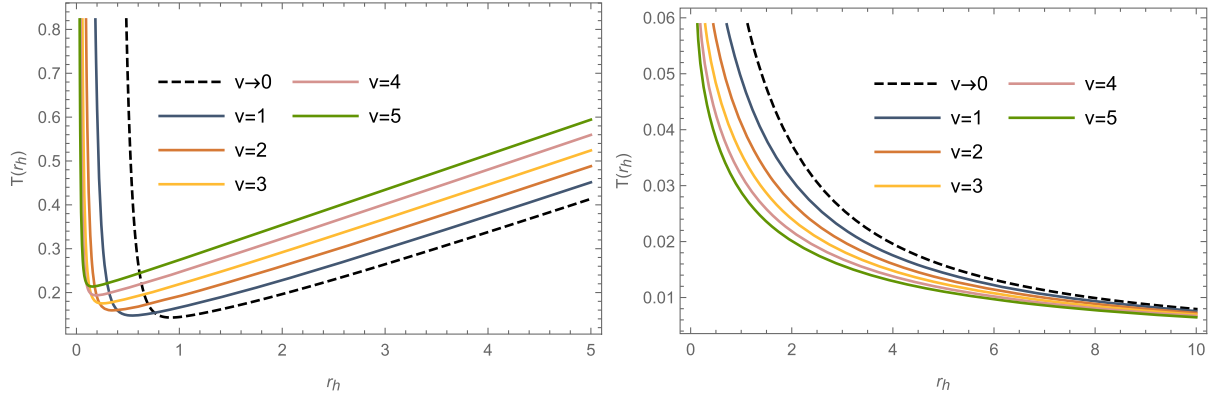
FIG. 8. The temperature of the hairy black hole configurations for asymptotically AdS $\Lambda_{\text{eff}} = -1$ (left) and flat $\Lambda_{\text{eff}} = 0$ (right) spacetimes, where we have fixed $Q_m = 0.5$, $\alpha = 0.5$, while changing the scalar charge ν.

$$S(r_h) = 2\pi\mathcal{A}, \tag{40}$$

where $\mathcal{A} = 4\pi[b_1(r_h)]^2$ is the area of the black hole. Hence

$$S(r_h) = 8\pi^2 r_h(r_h + \nu), \tag{41}$$

with the scalar charge appearing in the entropy, resulting in higher entropy in comparison with the nonhairy black hole, since $\nu > 0$.

To study the possibility of phase transitions, we will calculate the heat capacity. A positive heat capacity indicates that the black hole is thermodynamically stable. Nonstable black holes may undergo a phase transition in order to be stabilized. Phase transitions occur at the points where the heat capacity vanishes or diverges. A vanishing point in the heat capacity indicates a first order phase transition, while a divergence point indicates a second order phase transition. The first order phase transition occurs at high Gibbs energy and it does not change the favored configuration while a second order phase transition occurs at lower Gibbs energy and allows the coexistence of two configurations.

The heat capacity is given by

$$C(r_h) = \left.\frac{\partial m}{\partial T}\right|_{r=r_h} = \frac{m'(r_h)}{T'(r_h)}, \tag{42}$$

where $m(r_h)$ is the mass as a function of the event horizon of the black hole, obtained from the relation $b(r_h) = 0$. The explicit expression is too complicated to be given here. For AdS spacetime, for large r_h, the heat capacity is positive, since

$$C(r_h \gg 1) \sim 2\pi r_h^2 + 2\pi\nu r_h + \frac{\pi(\nu^2\Lambda_{\text{eff}} - 20)}{5\Lambda_{\text{eff}}} + \mathcal{O}\left(\frac{1}{r_h^2}\right), \tag{43}$$

and the AdS black holes are stable. However, in order to see if the black hole undergoes a phase transition before it gets stabilized we will plot the heat capacity in Fig. 9. The fact is that the asymptotically AdS Euler-Heisenberg hairy black holes undergo a second order phase transition and then they are stabilized. The phase transition point occurs at
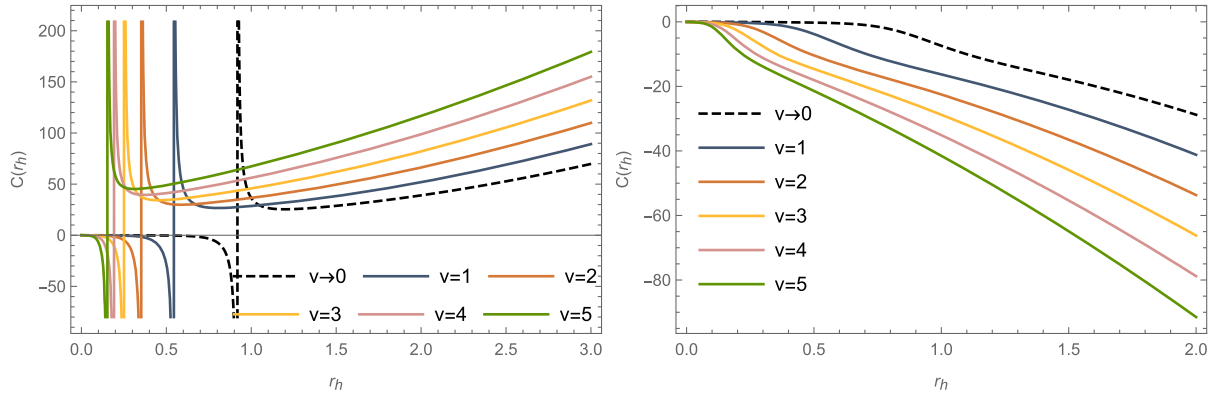

FIG. 9. The heat capacity for asymptotically AdS $\Lambda_{\text{eff}} = -1$ and flat $\Lambda_{\text{eff}} = 0$ spacetimes, where we have fixed $Q_m = 0.5$, $\alpha = 0.5$, while changing the scalar charge ν.

the minima of temperature. For a flat spacetime, the heat capacity asymptotes to

$$C(r_h \gg 1) \sim -2\pi r_h^2 - 2(\pi\nu)r_h + \mathcal{O}\left(\frac{1}{r_h^2}\right), \quad (44)$$

where we can see that the flat black holes are thermodynamically unstable and there exists no phase transition to make the black holes stable as we can deduce from Fig. 9.

V. ENERGY CONDITIONS

In this section we will discuss the energy conditions of the hairy black hole. For this reason, we will use the Einstein equation in the appropriate reference frame, where we can identify the energy density, the radial and tangential pressure as

$$G^{\mu}{}_{\nu} = T^{\mu}{}_{\nu}, \quad (45)$$

$$\rho = -T^{t}{}_{t}, \quad (46)$$

$$p_r = T^{r}{}_{r}, \quad (47)$$

$$p_{\theta} = p_{\varphi} = T^{\theta}{}_{\theta}. \quad (48)$$

The weak energy condition (WEC) states that given a timelike vector field t^a, the quantity $T_{ab}t^a t^b$ is positive, i.e., $T_{ab}t^a t^b \geq 0 \to \rho \geq 0$. The null energy condition (NEC) states that $T_{ab}l^a l^b \geq 0 \to \rho + p_r > 0$, where $l^a l_a = 0$, so that the geometry will have a focusing effect on null geodesics. For the energy momentum tensor of the scalar field, we have

$$\rho^{\phi} = \frac{1}{2}b(r)\phi'(r)^2 + V(r) = -p_{\theta}^{\phi}, \quad (49)$$

$$p_r^{\phi} = \frac{1}{2}b(r)\phi'(r)^2 - V(r), \quad (50)$$

while for the energy momentum tensor of the Euler-Heisenberg theory we obtain

$$
\begin{aligned}
\rho^{EM} = &-\frac{2\alpha Q_m^4}{b_1(r)^8} + \frac{Q_m^2(1 - 4(\alpha - 32\beta)\mathcal{A}'(r)^2)}{b_1(r)^4} \\
&+ \frac{4\beta Q_m \mathcal{A}'(r)}{b_1(r)^2} + 6\alpha\mathcal{A}'(r)^4 + \mathcal{A}'(r)^2 = -p_r^{EM},
\end{aligned}
$$
$$(51)$$

$$
\begin{aligned}
p_{\theta}^{EM} = &-\frac{6\alpha Q_m^4}{b_1(r)^8} + \frac{Q_m^2(4(\alpha - 32\beta)\mathcal{A}'(r)^2 + 1)}{b_1(r)^4} \\
&- \frac{4\beta Q_m \mathcal{A}'(r)}{b_1(r)^2} + 2\alpha\mathcal{A}'(r)^4 + \mathcal{A}'(r)^2.
\end{aligned}
$$
$$(52)$$

We will at first discuss the NEC, which implies $\rho + p_r \geq 0$. By adding the energy densities and radial pressures, we have

$$
\begin{aligned}
\rho + p_r &= \rho^{\phi} + \rho^{EM} + p_r^{\phi} + p_r^{EM} \\
&= \rho^{\phi} - p_r^{EM} + p_r^{\phi} + p_r^{EM} = b(r)\phi'(r)^2. \quad (53)
\end{aligned}
$$

First of all $\phi'(r)^2 > 0$ for any $r > 0$. $b(r)$ is negative inside the black hole, resulting in the violation of the NEC, zero at the event horizon resulting to $\rho + p_r = 0$, while after the event horizon $b(r)$ is positive, hence, the NEC is protected, regardless of the asymptotic nature of spacetime. For the contribution of the scalar field to the total energy density, we can see that inside the event horizon, where $b(r) < 0$, the WEC is violated by the scalar field, since $V(r)$ is also negative, i.e., $V(r) < 0$ regardless of the asymptotic nature of spacetime. On the event horizon $b(r_h) = 0$ and since $V(r_h) < 0$ the WEC is also violated. Caution must be given for the contribution of the scalar field to the energy density in the causal region of the black hole, i.e., $r > r_h$. For asymptotically AdS spacetimes, outside of the event horizon we have $b(r) > 0$ and $V(r) < 0$, however, the scalar potential is too negative, hence as we can see in Fig. 10, the scalar field part of the energy momentum tensor will always violate the WEC. For the asymptotically flat case, at large distances, the kinetic energy of the scalar field $\mathcal{T}(r) = b(r)\phi'(r)^2/2$ asymptotes to

$$\mathcal{T}(r \to \infty) \sim \frac{\nu^2}{4r^4} + \frac{-5\nu^3 - 7m\nu^2}{10r^5} + \mathcal{O}\left(\left(\frac{1}{r}\right)^6\right), \quad (54)$$

while the potential behaves as

$$V(r \to \infty) \sim -\frac{m\nu^2}{5r^5} + \mathcal{O}\left(\left(\frac{1}{r}\right)^6\right). \quad (55)$$

It is clear that their sum $\mathcal{T}(r) + V(r)$ will be positive at large distances, since the kinetic energy surpasses the contribution of the potential. It is therefore evident that for a region outside of the black hole horizon $\rho^{\phi} > 0$. The electromagnetic part of the energy density yields

$$\rho^{EM}(r) = \frac{Q_m^2}{r^2(\nu + r)^2} - \frac{2\alpha Q_m^4}{r^4(\nu + r)^4}. \quad (56)$$

There will be regions of negative energy density due to the Euler-Heisenberg modified electromagnetism parameter α. We plot $\rho^{EM}(r)$ in Fig. 10 where we can see that $\rho^{EM}(r)$ can be positive, however it does not contribute much in the total energy density, hence $\rho < 0$ everywhere and the WEC is violated in the case of AdS spacetime. However in the asymptotically flat case, it is obvious from (54), (55) and FIG. 10, that, for a region outside of the event horizon to infinity $\rho > 0$ and the WEC holds.
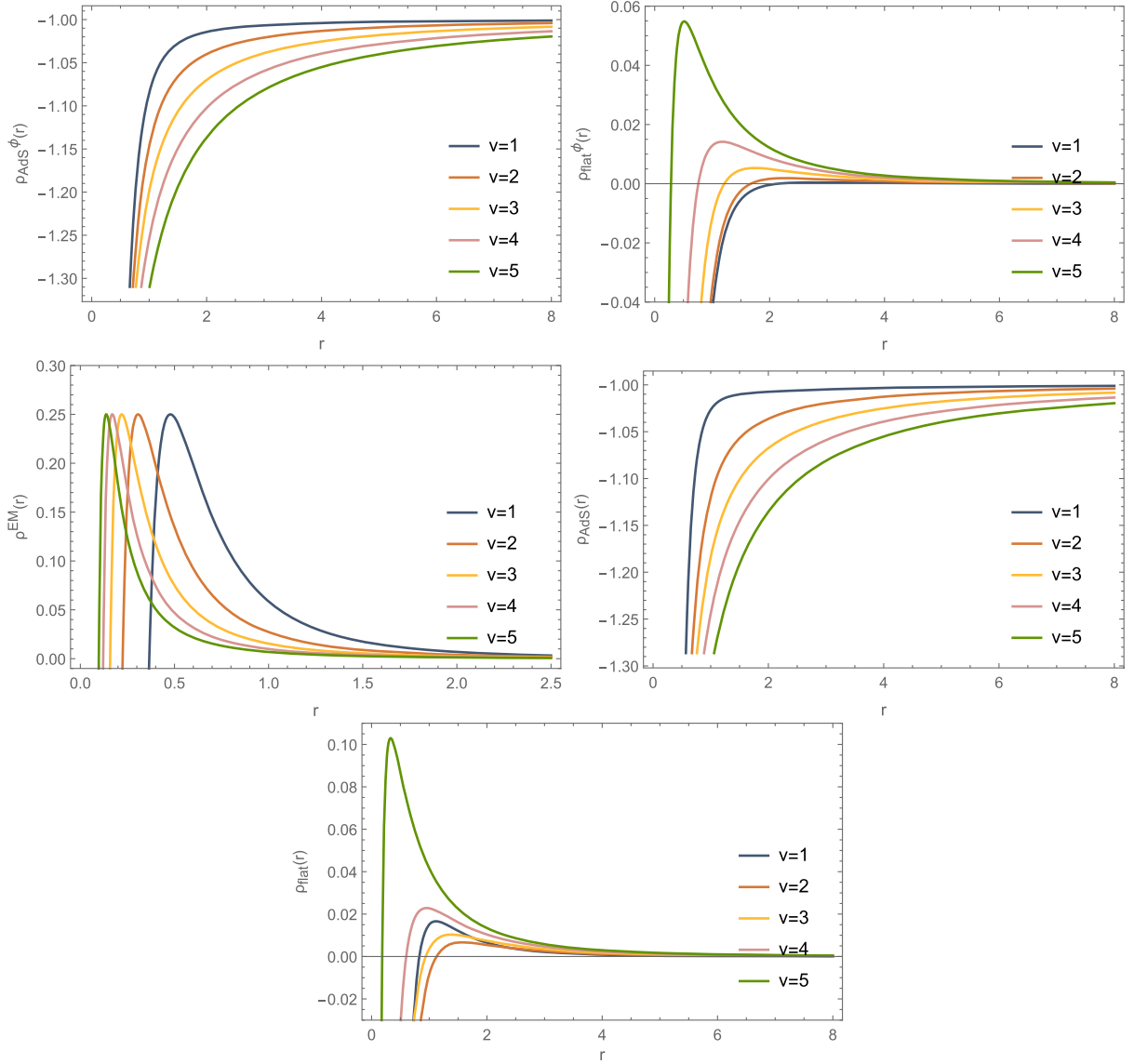
FIG. 10. Several energy densities are plotted. In the first row, we have the energy density of the scalar field for AdS (left) and flat spacetimes (right). In the second row, we plot the energy density of the electromagnetic part of the energy momentum tensor (left) and the total energy density for AdS spacetime (right). In the third row we plot the total energy density of the asymptotically flat case. For the AdS cases we have set $\Lambda_{\text{eff}} = -1$, for the flat spacetimes $\Lambda_{\text{eff}} = 0$, while we have fixed $m = 1$, $Q_m = 0.5$, $\alpha = 0.5$, and we vary the scalar charge ν.

VI. CONCLUSIONS

We studied the Einstein-Euler-Heisenberg theory in the presence of a minimally coupled to gravity, self interacting scalar field. We solved analytically the field equations and, assuming an electromagnetic field with magnetic charge, we obtained novel magnetically charged hairy black holes. The scalar field dresses the black hole with secondary scalar hair, while the scalar potential is negative in order to support the hairy structure and it possesses a mass term that satisfies the Breitenlohner-Freedman bound that ensures the perturbative stability of the AdS spacetime. The presence of the scalar charge is introducing a new scale in the theory which leads to

the appearance of an effective cosmological constant. The hairy black hole develops three horizons when Euler-Heisenberg parameter and the magnetic charge Q_m are small and the horizon radius is getting large when the scalar charge and the gravitational mass are large.

We also studied the thermodynamics of the hairy Euler-Heisenberg black hole. We found that the presence of matter outside the horizon of the black hole increases the temperature only for small black holes. Also we found the same behavior for the magnetic field, it increases the temperature only for small black holes. Calculating the heat capacity we found that the asymptotically AdS Euler-Heisenberg hairy black hole undergoes a second order

phase transition and then it is stabilized. The phase transition point occurs at the minimum of the temperature while the scalar field gains entropy for the black hole by the addition of a linear term in the entropy and hence the hairy black holes are thermodynamically preferred.

We found that the WEC is violated on the horizon of the hairy Euler-Heisenberg black hole. For asymptotically AdS spacetimes, outside of the event horizon the scalar field part of the energy momentum tensor will always violate the WEC. However in the asymptotically flat case, we found that for a region outside of the event horizon to infinity the WEC holds.

It would be interesting to extend this work to the case that the scalar field is magnetically charged. Then we expect that the magnetized scalar field will interact with the magnetic field, so that the magnetized scalar charge, the magnetic charge and the Euler-Heisenberg parameter will play a decisive role in the structure and properties of the magnetized hairy Euler-Heisenberg black hole. It would also be of interest to study the shadow of the obtained spacetime and to constrain the modified Euler-Heisenberg parameter along with the scalar charge from the results of the Event Horizon Telescope [74] in the astrophysical scenario $Q_m \ll m$. In [75] it was found that considering Maxwell electrodynamics there is a threshold value for the electric charge Q, above which any value of the scalar charge is allowed. It would be worth investigating the same possibility in our case.

[1] J. D. Bekenstein, Transcendence of the Law of Baryon-Number Conservation in Black Hole Physics, Phys. Rev. Lett. **28,** 452 (1972).

[2] J. D. Bekenstein, Nonexistence of baryon number for black holes, Phys. Rev. D **5,** 2403 (1972).

[3] C. A. R. Herdeiro and E. Radu, Asymptotically flat black holes with scalar hair: A review, Int. J. Mod. Phys. D **24,** 1542014 (2015).

[4] N. Bocharova, K. Bronnikov, and V. Melnikov, An exact solution of the system of Einstein equations and mass-free scalar field, Vestn. Mosk. Univ., Ser. 3: Fiz., Astron. **6,** 706 (1970); J. D. Bekenstein, Exact solutions of Einstein-conformal scalar equations, Ann. Phys. (N.Y.) **82,** 535 (1974); Black holes with scalar charge, Ann. Phys. (N.Y.) **91,** 75 (1975).

[5] K. A. Bronnikov and Y. N. Kireyev, Instability of black holes with scalar charge, Phys. Lett. **67A,** 95 (1978).

[6] C. Martinez, R. Troncoso, and J. Zanelli, De Sitter black hole with a conformally coupled scalar field in four-dimensions, Phys. Rev. D **67,** 024008 (2003).

[7] T. J. T. Harper, P. A. Thomas, E. Winstanley, and P. M. Young, Instability of a four-dimensional de Sitter black hole with a conformally coupled scalar field, Phys. Rev. D **70,** 064023 (2004).

[8] T. Karakasis, E. Papantonopoulos, Z. Y. Tang, and B. Wang, Exact black hole solutions with a conformally coupled scalar field and dynamic Ricci curvature in f(R) gravity theories, Eur. Phys. J. C **81,** 897 (2021).

[9] C. Martinez, R. Troncoso, and J. Zanelli, Exact black hole solution with a minimally coupled scalar field, Phys. Rev. D **70,** 084035 (2004).

[10] C. Martinez and R. Troncoso, Electrically charged black hole with scalar hair, Phys. Rev. D **74,** 064007 (2006).

[11] T. Kolyvaris, G. Koutsoumbas, E. Papantonopoulos, and G. Siopsis, A new class of exact hairy black hole solutions, Gen. Relativ. Gravit. **43,** 163 (2011).

[12] P. A. González, E. Papantonopoulos, J. Saavedra, and Y. Vásquez, Four-dimensional asymptotically AdS black holes with scalar hair, J. High Energy Phys. 12 (2013) 021.

[13] P. A. González, E. Papantonopoulos, J. Saavedra, and Y. Vásquez, Extremal hairy black holes, J. High Energy Phys. 11 (2014) 011.

[14] J. Barrientos, P. A. González, and Y. Vásquez, Four-dimensional black holes with scalar hair in nonlinear electrodynamics, Eur. Phys. J. C **76,** 677 (2016).

[15] A. Rahmani, M. Khodadi, M. Honardoost, and H. R. Sepangi, Instability and no-hair paradigm in d-dimensional charged-AdS black holes, Nucl. Phys. **B960,** 115185 (2020).

[16] M. Khodadi, G. Lambiase, and D. F. Mota, No-hair theorem in the wake of Event Horizon Telescope, J. Cosmol. Astropart. Phys. 09 (2021) 028.

[17] R. A. Konoplya and A. Zhidenko, Shadows of parametrized axially symmetric black holes allowing for separation of variables, Phys. Rev. D **103,** 104033 (2021).

[18] A. Anabalon and A. Cisterna, Asymptotically (anti) de Sitter black holes and wormholes with a self interacting scalar field in four dimensions, Phys. Rev. D **85,** 084035 (2012).

[19] T. Kolyvaris, G. Koutsoumbas, E. Papantonopoulos, and G. Siopsis, Phase transition to a hairy black hole in asymptotically flat spacetime, J. High Energy Phys. 11 (2013) 133.

[20] T. Kolyvaris, G. Koutsoumbas, E. Papantonopoulos, and G. Siopsis, Scalar hair from a derivative coupling of a scalar field to the Einstein tensor, Classical Quantum Gravity **29,** 205011 (2012).

[21] M. Rinaldi, Black holes with non-minimal derivative coupling, Phys. Rev. D **86,** 084048 (2012).

[22] E. Papantonopoulos, Effects of the kinetic coupling of matter to curvature, Int. J. Mod. Phys. D **28,** 1942007 (2019).

[23] M. Minamitsuji, Solutions in the scalar-tensor theory with nonminimal derivative coupling, Phys. Rev. D **89,** 064017 (2014).

[24] A. Anabalon, A. Cisterna, and J. Oliva, Asymptotically locally AdS and flat black holes in Horndeski theory, Phys. Rev. D **89,** 084050 (2014).

[25] A. Cisterna and C. Erices, Asymptotically locally AdS and flat black holes in the presence of an electric field in the Horndeski scenario, Phys. Rev. D **89,** 084038 (2014).

[26] G. W. Horndeski, Second-order scalar-tensor field equations in a four-dimensional space, Int. J. Theor. Phys. **10,** 363 (1974).

[27] E. Babichev and C. Charmousis, Dressing a black hole with a time-dependent Galileon, J. High Energy Phys. 08 (2014) 106.

[28] E. Babichev, C. Charmousis, and A. Lehébel, Asymptotically flat black holes in Horndeski theory and beyond, J. Cosmol. Astropart. Phys. 04 (2017) 027.

[29] C. Charmousis, T. Kolyvaris, E. Papantonopoulos, and M. Tsoukalas, Black holes in bi-scalar extensions of Horndeski theories, J. High Energy Phys. 07 (2014) 085.

[30] E. Babichev, C. Charmousis, and M. Hassaine, Charged Galileon black holes, J. Cosmol. Astropart. Phys. 05 (2015) 031.

[31] M. Bravo-Gaete and M. Hassaine, Lifshitz black holes with a time-dependent scalar field in a Horndeski theory, Phys. Rev. D **89,** 104028 (2014).

[32] M. Bravo-Gaete and M. Hassaine, Thermodynamics of a BTZ black hole solution with an Horndeski source, Phys. Rev. D **90,** 024008 (2014).

[33] P. Kanti, N. E. Mavromatos, J. Rizos, K. Tamvakis, and E. Winstanley, Dilatonic black holes in higher curvature string gravity, Phys. Rev. D **54,** 5049 (1996).

[34] T. P. Sotiriou and S. Y. Zhou, Black Hole Hair in Generalized Scalar-Tensor Gravity, Phys. Rev. Lett. **112,** 251102 (2014).

[35] T. P. Sotiriou and S. Y. Zhou, Black hole hair in generalized scalar-tensor gravity: An explicit example, Phys. Rev. D **90,** 124063 (2014).

[36] G. Antoniou, A. Bakopoulos, and P. Kanti, Evasion of No-Hair Theorems and Novel Black-Hole Solutions in Gauss-Bonnet Theories, Phys. Rev. Lett. **120,** 131102 (2018).

[37] D. D. Doneva and S. S. Yazadjiev, New Gauss-Bonnet Black Holes with Curvature-Induced Scalarization in Extended Scalar-Tensor Theories, Phys. Rev. Lett. **120,** 131103 (2018).

[38] H. O. Silva, J. Sakstein, L. Gualtieri, T. P. Sotiriou, and E. Berti, Spontaneous Scalarization of Black Holes and Compact Stars from a Gauss-Bonnet Coupling, Phys. Rev. Lett. **120,** 131104 (2018).

[39] D. D. Doneva, S. Kiorpelidi, P. G. Nedkova, E. Papantonopoulos, and S. S. Yazadjiev, Charged Gauss-Bonnet black holes with curvature induced scalarization in the extended scalar-tensor theories, Phys. Rev. D **98,** 104056 (2018).

[40] D. Garfinkle, G. T. Horowitz, and A. Strominger, Charged black holes in string theory, Phys. Rev. D **43,** 3140 (1991); Erratum, Phys. Rev. D **45,** 3888 (1992).

[41] A. Anabalon, D. Astefanesei, and R. Mann, Exact asymptotically flat charged hairy black holes with a dilaton potential, J. High Energy Phys. 10 (2013) 184.

[42] D. Astefanesei, D. Choque, F. Gómez, and R. Rojas, Thermodynamically stable asymptotically flat hairy black holes with a dilaton potential, J. High Energy Phys. 03 (2019) 205.

[43] G. W. Gibbons, Antigravitating black hole solitons with scalar hair in $N = 4$ supergravity, Nucl. Phys. **B207,** 337 (1982).

[44] S. Priyadarshinee, S. Mahapatra, and I. Banerjee, Analytic topological hairy dyonic black holes and thermodynamics, Phys. Rev. D **104,** 084023 (2021).

[45] S. Yu, J. Qiu, and C. Gao, Constructing black holes in Einstein–Maxwell-scalar theory, Classical Quantum Gravity **38,** 105006 (2021).

[46] Z. Y. Tang, B. Wang, T. Karakasis, and E. Papantonopoulos, Curvature scalarization of black holes in f(R) gravity, Phys. Rev. D **104,** 064017 (2021).

[47] T. Karakasis, E. Papantonopoulos, Z. Y. Tang, and B. Wang, Black holes of $(2 + 1)$-dimensional $f(R)$ gravity coupled to a scalar field, Phys. Rev. D **103,** 064063 (2021).

[48] T. Karakasis, E. Papantonopoulos, Z. Y. Tang, and B. Wang, $(2 + 1)$-dimensional black holes in f(R,ϕ) gravity, Phys. Rev. D **105,** 044038 (2022).

[49] W. Heisenberg and H. Euler, Consequences of Dirac's theory of positrons, Z. Phys. **98,** 714 (1936).

[50] Y. N. Obukhov and G. F. Rubilar, Fresnel analysis of the wave propagation in nonlinear electrodynamics, Phys. Rev. D **66,** 024042 (2002).

[51] G. Brodin, M. Marklund, and L. Stenflo, Proposal for Detection of QED Vacuum Nonlinearities in Maxwell's Equations by the Use of Waveguides, Phys. Rev. Lett. **87,** 171801 (2001).

[52] H. Yajima and T. Tamaki, Black hole solutions in Euler-Heisenberg theory, Phys. Rev. D **63,** 064007 (2001).

[53] R. Ruffini, Y. B. Wu, and S. S. Xue, Einstein-Euler-Heisenberg theory and charged black holes, Phys. Rev. D **88,** 085004 (2013).

[54] D. Amaro and A. Macías, Geodesic structure of the Euler-Heisenberg static black hole, Phys. Rev. D **102,** 104054 (2020).

[55] D. Chen and C. Gao, Circular motion and chaos bound of charged particles around Einstein-Euler-Heisenberg AdS black hole, arXiv:2205.08337.

[56] D. Magos and N. Bretón, Thermodynamics of the Euler-Heisenberg-AdS black hole, Phys. Rev. D **102,** 084011 (2020).

[57] H. Dai, Z. Zhao, and S. Zhang, Thermodynamic phase transition of Euler-Heisenberg-AdS black hole on free energy landscape, arXiv:2202.14007.

[58] N. Bretón and L. A. López, Birefringence and quasinormal modes of the Einstein-Euler-Heisenberg black hole, Phys. Rev. D **104,** 024064 (2021).

[59] N. Bretón, C. Lämmerzahl, and A. Macías, Rotating black holes in the Einstein–Euler–Heisenberg theory, Classical Quantum Gravity **36,** 235022 (2019).

[60] N. Bretón, C. Lämmerzahl, and A. Macías, Rotating structure of the Euler-Heisenberg black hole, Phys. Rev. D **105,** 104046 (2022).

[61] I. Z. Stefanov, S. S. Yazadjiev, and M. D. Todorov, Scalar-tensor black holes coupled to Euler-Heisenberg nonlinear electrodynamics, Mod. Phys. Lett. A **22,** 1217 (2007).

[62] M. Guerrero and D. Rubiera-Garcia, Nonsingular black holes in nonlinear gravity coupled to Euler-Heisenberg electrodynamics, Phys. Rev. D **102**, 024005 (2020).

[63] G. G. L. Nashed and S. Nojiri, Mimetic Euler-Heisenberg theory, charged solutions, and multihorizon black holes, Phys. Rev. D **104**, 044043 (2021).

[64] A. Allahyari, M. Khodadi, S. Vagnozzi, and D. F. Mota, Magnetically charged black holes from non-linear electrodynamics and the Event Horizon Telescope, J. Cosmol. Astropart. Phys. 02 (2020) 003.

[65] M. Zajaček, A. Tursunov, A. Eckart, and S. Britzen, On the charge of the Galactic centre black hole, Mon. Not. R. Astron. Soc. **480**, 4408 (2018).

[66] J. Maldacena, Comments on magnetic black holes, J. High Energy Phys. 04 (2021) 079.

[67] M. A. Melvin, Pure magnetic and electric geons, Phys. Lett. **8**, 65 (1964).

[68] M. A. Melvin, Dynamics of cylindrical electromagnetic universes, Phys. Rev. **139**, B225 (1965).

[69] K. S. Thorne, Energy of infinitely long, cylindrically symmetric systems in general relativity, Phys. Rev. **138**, B251 (1965).

[70] K. S. Thorne, Absolute stability of Melvin's magnetic universe, Phys. Rev. **139**, B244 (1965).

[71] P. Breitenlohner and D. Z. Freedman, Stability in gauged extended supergravity, Ann. Phys. (N.Y.) **144**, 249 (1982).

[72] R. M. Wald, Black hole entropy is the Noether charge, Phys. Rev. D **48**, R3427 (1993).

[73] R. Brustein, D. Gorbonos, and M. Hadad, Wald's entropy is equal to a quarter of the horizon area in units of the effective gravitational coupling, Phys. Rev. D **79**, 044025 (2009).

[74] K. Akiyama *et al.* (Event Horizon Telescope Collaboration), First M87 Event Horizon Telescope results. I. The shadow of the supermassive black hole, Astrophys. J. Lett. **875**, L1 (2019).

[75] M. Khodadi, A. Allahyari, S. Vagnozzi, and D. F. Mota, Black holes with scalar hair in light of the Event Horizon Telescope, J. Cosmol. Astropart. Phys. 09 (2020) 026.